Available online at www.sciencedirect.com
ScienceDirect
Catalysis Today 133–135 (2008) 244–254
CATALYSIS TODAY
www.elsevier.com/locate/cattod

Oxidative desulfurization of synthetic diesel using supported catalysts Part III. Support effect on vanadium-based catalysts

Luis Cedeño-Caero *, Hilda Gomez-Bernal, Adriana Fraustro-Cuevas, Hector D. Guerra-Gomez, Rogelio Cuevas-Garcia

UNICAT, Facultad de Química, Universidad Nacional Autónoma de México, Cd. Universitaria 04510, México D.F., Mexico

Available online 31 January 2008

Abstract

Oxidesulfurization (ODS) of benzothiophenic compounds prevailing in diesel was conducted with hydrogen peroxide in presence of various catalysts, using a model diesel and actual diesel fuel. ODS activities of dibenzothiophenes (DBTs) in hexadecane for a series of V_2O_5 catalysts supported on alumina, titania, ceria, niobia and silica, were evaluated. Results show that the oxidation activity of DBTs depends on the support used. It was observed that the sulfone yield is not proportional to textural properties or V content. For all catalysts, ODS of benzothiophene (BT), dibenzothiophene (DBT), 4-methyl dibenzothiophene (4-MDBT) and 4,6-dimethyl dibenzothiophene (4,6-DMDBT) decreased in the following order: DBT > 4-MDBT > 4,6-DMDBT > BT. This trend does not depend on the catalyst used or the textural properties of the catalysts and supports. In presence of indole ODS activities diminish, except with catalysts supported on alumina-titania mixed oxide, whereas with V_2O_5/TiO_2 catalyst the performance is the highest. ODS of Mexican diesel fuel was carried out in presence of this catalyst and S level was diminished in about 99%.

Keywords: Oxidative desulfurization; Dibenzothiophenes; V_2O_5 supported catalysts; Support effect; Thermal spreading; Diesel; Preparation method

1. Introduction

Although hydrodesulfurization (HDS) process has dominated desulfurization of liquid fuels, their cost and the emergence of more stringent fuel specifications now combine to motivate the development of alternate processes. Petroleum refiners will confront the need of a hydrogen plant, an HDS plant, a Claus sulfur plant and tail gas cleanup. Unit costs of these processing facilities tend to increase dramatically with scale up of capacity in accordance with standard engineering principles. Within a few years, liquid fuel specifications are forecast to be moving towards sulfur levels in the range of 50–10 ppm worldwide [1,2]. It is relatively easy to remove the majority of sulfur present as simple sulfides, disulfides and mercaptans, comparatively inexpensive processes can accomplish this goal. Considerably more difficult are benzothiophenic compounds, especially dibenzothiophene (DBT) and their many substituted homologues. For these reasons, several groups are exploring alternate desulfurization processes for gasoline, diesel and other liquid fuels. These include direct adsorption, bioprocessing and oxidation [1]. In this paper we explore the application of oxidesulfurization (ODS) as a viable alternative to obtain ultra low-sulfur diesel (ULSD), using this process as a HDS post-treatment.

ODS is a current process and has been discussed recently in previous publications [3–19]. The advantage that ODS has over conventional HDS is that the difficult-to-desulfurize, refractory-substituted dibenzothiophenes (DBTs), are easily oxidized under low temperature and pressure conditions to form the corresponding sulfones. Organic peroxides can supply oxidant species and there is no hydrogen consumed in this reaction. Sulfones are highly polar compounds and are easily separated from the fuel product by extraction. Sulfur compounds such as disulfides are easy to hydrodesulfurize, but oxidize slowly. For this reason, ODS can be utilized as a second stage after existing HDS unit, taking a low sulfur diesel (~500 ppm) down to ULSD (<10 ppm) levels. In this situation, the diesel product has been depleted of difficult-

* Corresponding author.
E-mail address: caero@servidor.unam.mx (L. Cedeño-Caero).

0920-5861/$ – see front matter © 2007 Elsevier B.V. All rights reserved.
doi:10.1016/j.cattod.2007.12.017

to-oxidize sulfur species and has a high concentration of the most refractory DBTs constituents.

ODS in presence of a solid catalyst and extraction solvent is defined in two consecutive steps [17]: removal of sulfur compounds by extraction from the treated fuel, and the following step is their oxidation to the corresponding sulfones in the solvent phase, since having reactants in the polar phase facilitates their reaction. Thus the solvent is very important in the process, it was reported [17] that the S-compounds can be extracted from fuels with polar solvents, but it has been observed that without the solvent no oxidation reaction of these compounds in a few minutes (<60 min) is obtained. Then, total removal depends on the contribution of extraction and oxidation steps.

In our recent studies [16–18], vanadium supported catalysts (V_2O_5/TiO_2 and V_2O_5/Al_2O_3) were used to evaluate several effects on ODS, such as extraction solvent, oxidant reagent, reaction temperature and process conditions. ODS of dibenzothiophenes (DBTs) was performed using a batch reaction system. The results indicated that total removal depends on the catalytic support used, TiO_2 or Al_2O_3. DBT total removal reached 99.9% at 60 °C with V_2O_5/TiO_2 catalyst and H_2O_2 as oxidant, and the most refractory compound in ODS (4,6-DMDBT) reached 82.2%. In these conditions, using V_2O_5/Al_2O_3 as catalyst, the total removal was 99.9 and 93.5% for DBT and 4,6-DMDBT, respectively.

N-compounds prevailing in fuels is another important aspect on ODS reactions. Otsuki et al. [20] studied the effect of nitrogen-model compounds, olefins, aliphatic and aromatic hydrocarbons, found in light gas oil, on oxidation of DBT. This study shows that the conversion of DBT was not influenced by the addition of *n*-pentadecane or by addition of xylene, indicating that aliphatic and aromatic compounds did not affect the oxidation of DBT. In contrast, the addition of di-isobutylene and indole retarded the oxidation reaction. These results were attributed to a higher reactivity of these compounds compared to that of DBT, in conditions of the oxidation reaction. Ishihara et al. [21] reported that denitrogenation performance of N-containing compounds in oxidation process is possible. Denitrogenation activity order of model compounds was: indole > quinoline > acridine > carbazole. However, while the oxidation products of N-compounds were not fully identified, they suggested the presence of polymeric compounds. Taking into account that sulfur compounds are removed quantitatively from fuels by physical extraction without oxidation reaction [17], then the N-compounds could also have been removed only by extraction. In previous work [18] we found that the ODS activity, of DBTs in presence of N-compounds, decreases in the order: quinoline > indole > carbazole. Since only indole is oxidized in these conditions and all N-compounds inhibited ODS reaction, this poisoning effect was attributed not only to competitive adsorption between sulfur and nitrogen compounds for catalytic sites, but also to their basic character.

In order to improve ODS activity of vanadium catalyst; the current research focuses on the use of different types of supports, and from this point of view it will be interesting to evaluate the performance of recently discovered SBA-15 mesoporous silica material. SBA-15 is a high surface area ordered mesoporous support with controlled pore size [22,23], and these characteristics make them very promising for application in oil refining. It is formed by reacting micelles of surfactant with a silica source: their interaction leads to the precipitation of an organized mesophase, and after polymerization of the silica precursor and calcination, an ordered porous structure is obtained. Depending on the choice of the surfactant and on synthesis conditions, mesoporous materials with honeycomb structure and controlled pore size in the range 6–9 nm can be obtained. The rather thin walls of this silica support (ca. 3 nm) allow them to develop very high surface areas (ca. 800 m^2/g).

The conventional method for the preparation of V supported catalysts is the incipient wetness impregnation (IWI) with ammonium metavanadate solutions, followed by calcination [24]. However, thermal spreading (TS) is of special interest, because it is very simple to achieve. TS method is the spontaneous dispersion over macroscopic distances of a metal oxide onto the surface of an oxide support during extensive thermal treatment. It leads to the formation of a monolayer or sub-monolayer of the spread oxide. TS of V_2O_5 is known to occur on many supports, and among them Al_2O_3 is the most widely studied [25]. Although many different synthesis methods have been used in preparing supported vanadium oxide catalysts, all supported vanadium oxide catalysts were found to contain essentially the same vanadium oxide configurations after prolonged calcination treatments [26]. This means that the preparation method does not influence the local coordination environment of supported vanadium oxides. But it is possible that bond strength of vanadia–support changes with the preparation method.

In this work, V_2O_5/TiO_2 catalysts with various V loadings were prepared by TS and by IWI in order to compare the preparation method effect. The influence of these methods was evaluated on textural properties, dispersion of vanadium species by SEM–EDX, XRD and Raman spectroscopy, and on ODS reactivity of benzothiophenic compounds prevailing in diesel. Then, we report results obtained on ODS of a model and actual diesel, in presence of vanadium supported catalyst. Firstly several oxide supports were tested, such as ceria, alumina, titania, silica (SBA-15), niobia and mixed oxides as alumina–titania and silica–alumina. After, N-compound (indole) effect on ODS reaction with these catalysts was evaluated. Finally we evaluated the ODS of actual Mexican diesel fuel with the best catalysts used.

2. Experimental

2.1. Materials

All compounds were purchased from Sigma/Aldrich and used without further treatment. Benzothiophenes, which represent sulfur species in diesel, were selected to evaluate reactivity in ODS. Hexadecane (99.8%) was used as solvent of model compounds: benzothiophene (BT, 98%), dibenzothio-

phene (DBT, 98%), 4-methyl dibenzothiophene (4-MDBT, 96%) and 4,6-dimethyl dibenzothiophene (4,6-DMDBT, 97%). This synthetic diesel was prepared with 936 S ppmw: 308 of BT, 224 of DBT, 209 of 4-MDBT and 195 of 4,6-DMDBT. Acetonitrile (99.9%) was used as extraction solvent. Actual diesel was a commercial Mexican-diesel fuel with 350 ppm of total S, and with additional amounts of DBTs (800 and 1005 ppm of S total).

2.2. Preparation and characterization

V_2O_5/Al_2O_3, V_2O_5/TiO_2, V_2O_5/CeO_2, V_2O_5/SiO_2–Al_2O and V_2O_5/Al_2O_3–TiO_2 catalysts were obtained by thermal spreading (TS) at 500 °C during overnight in air [24,25]. They represent a physical mixture of the support and V_2O_5 (99.6%, Aldrich) obtained through intensive manual milling. Each catalyst was prepared with a V_2O_5 loading equivalent to a monolayer coverage [27,28], which corresponds to 0.1 wt.% of V_2O_5/m^2 of support. The catalysts prepared, their nomenclature and textural properties of the supports, are shown in Table 1. The supports used are commercial samples, except Al_2O_3 (5%)–TiO_2 (95%) mixed oxide, which was prepared by sol–gel method as described in [29].

Preparation of V*x*/Si catalysts. SBA-15 support was prepared as described elsewhere [22,23]. V-based catalysts were prepared by both methods, TS and incipient wetness impregnation (IWI). For the former, appropriate amounts of V_2O_5 and support were finely grounded together using a mortar during 30 min to ensure a homogeneous distribution. The mechanical mixture was thermally treated at 500 °C (heating rate 2 °C/min) during overnight under air. Additionally, V_2O_5/SBA-15 (V*x*/Si) catalyst was prepared by IWI of ammonium metavanadate (x = 5 and 10 wt.% of V_2O_5), dissolved in oxalic acid (2 M) on a synthesized SBA-15 (SBET = 861 m^2/g), followed by drying at 100 °C, during 24 h and calcination under air at 500 °C (5 h).

V*x*/Ti catalysts with various V_2O_5 loading (x = 5, 10, 12 and 15 wt.%) were prepared by TS, and by IWI in order to compare the preparation method effect. Catalysts of V_2O_5 supported on: Nb_2O_5 (V*x*/Nb) with various V_2O_5 loading (x = 2, 4, 6, 10 and 20 wt.%) and Al_2O_3–TiO_2 mixed oxide (V*x*/Al–Ti, x = 7.5, 15.0 and 22.5 wt.%) were also prepared by TS.

Catalysts were characterized by: X-ray diffraction (XRD) using a Siemens D500 powder diffractometer with Cu Kα radiation. The FT-Raman spectra of catalysts were performed in a Nicolet FT-Raman 950 spectrometer with a resolution of 4 cm^{-1} and 500 scans. Before the analysis, the samples were pretreated at 100 °C during 12 h in static air. Textural properties were obtained by N_2 adsorption–desorption isotherms of the samples, with a Tristar Micromeritics apparatus. Nitrogen physisorption isotherms were analyzed using the BJH method. Prior to the textural analysis, the samples were outgassed for 8 h in vacuum at 350 °C. Average pore size was evaluated from the desorption branch of the isotherm using the BJH model. Elemental composition was determined by SEM–EDX in a Jeol JSM-5900 LV microscope equipped with an energy dispersive X-ray (EDX) elemental analysis system. A conventional temperature programmed reduction (TPR) apparatus was used for the study of the reducibility of the catalysts. TPR of the catalysts was performed using a flow of H_2/Ar mixture (30% H_2 v/v, 25 cm^3/min) at atmospheric pressure, 0.25 g of sample and a heating rate of 10 °C/min from room temperature to 1000 °C.

2.3. Catalytic experiments

A batch reactor, fitted with a condenser, a mechanical stirrer and a thermocouple, was used to carry out the oxidation reaction. The reactor was immersed in a thermostatically controlled water bath to carry out the reactions at 60 °C. In a typical run, the water bath was first heated up and stabilized to the desired reaction temperature, and the mixture diesel–solvent (1:1 v/v) was added to the reactor. Then oxidant agent and catalyst were introduced into the reactor where the mixture was vigorous stirring. Reaction samples, from diesel and solvent phases, at 3, 10, 20, 30, and 60 min were withdrawn and injected (auto sampler) to the GC–FID after cooling to room temperature. GC–FID analyses were performed with an HP5890 Series II Gas Chromatograph with a PONA capillary column (Methyl silicone Gum, 50 m × 0.2 mm × 0.5 μm film thickness). Reactant and product identifications were achieved by comparing retention times in GC–FID and, from results obtained with a GC–PFPD (Varian CP-3800) and GC–MS (HP5890 Series II with MS detector). Tertbutyl hydroperoxide (70 wt.% TBHP) or hydrogen peroxide (30 wt.% H_2O_2) was used as oxidant (O/S = 4 initial ratio, mole/mole). TBHP was measured during reaction by standard permanganometric titration and GC–FID. H_2O_2 content was measured by standard iodometric titration. H_2O_2 was added in small doses to reduce thermal decomposition, according to previous results [16].

Table 1
Textural properties of supports and catalyst nomenclature

	Catalysts	Support area (m^2/g)	Pore volume (cm^3/g)	Average pore diameter (Å)
V/Al	V_2O_5/Al_2O_3	188	0.46	90
V/Ti	V_2O_5/TiO_2	120	0.38	130
V/Ce	V_2O_5/CeO_2	60	0.40	232
V/Nb	V_2O_5/Nb_2O_5	7	0.02	145
V/Al–Ti	V_2O_5/Al_2O_3(5%)–TiO_2(95%)	135	0.36	79
V/Si–Al	V_2O_5/SiO_2(87%)–Al_2O_3(13%)	661	0.84	41
V/Si	V_2O_5/SBA-15	861	0.99	75

Table 2
Textural properties and V loading of the catalysts

Catalyst	V_2O_5 (wt.%)	Surface area (m^2/g)	Pore volume (cm^3/g)	Average pore diameter (Å)
V19/Al	19.0	144	0.40	93
V6/Ce	6.0	29	0.15	208
V20/Nb	20.0	5	0.01	169
V22/Al–Ti	22.5	48	0.19	160
V15/Al–Ti	15.0	66	0.22	135
V7/Al–Ti	7.5	78	0.24	110
V10/Si	10.0	521	0.95	72
V5/Si	5.0	558	0.99	72

3. Results and discussion

First we will present the characterization results of the catalysts. Second, we will analyze the ODS activity of model S-compounds. Then, the effect of indole on ODS will be discussed, and finally, we will present the ODS of actual diesel with the best catalysts.

3.1. Characterization of catalysts

Surface areas of the catalysts are shown in Tables 2 and 3. These decrements in surface area of the catalysts respect to supports (Table 1) are due to penetration of V_2O_5 into the pores of the support during preparation step, covering the surface of the supports. For V/Al the area decreases 23%, but for other catalysts it diminishes significantly. This result is attributed to the obstruction of small pores since the pore average diameter increased, i.e. for V*x*/Ti from 130 to 274–379 Å. But, according to SEM–EDX results, a good surface distribution of V_2O_5 was obtained, except for catalysts based on silica. Fig. 1 shows a SEM–EDX micrograph of V/Si–Al, which presents clearly segregated phases of support (gray particles) and V_2O_5 (white particles). Similar results were obtained with V/Si catalysts, since TS is not a suitable method to support V on silica. Thus these catalysts were prepared by incipient wetness impregnation (IWI), which were obtained with good vanadia distribution.

Fig. 2 shows SEM–EDX elemental analysis map of V6/Nb catalyst, which shows a good distribution of V and Nb. Respectively, Tamman temperature of V_2O_5 and Nb_2O_5 are 370 and 620 °C [30] and V*x*/Nb catalysts were calcined at 500 °C, then the low Tamman temperature causes that the surface V species become very mobile and readily spread out over niobia. When V_2O_5 was incorporated on niobia, textural properties of V*x*/Nb catalysts were not modified appreciably, i.e. with V20/Nb the area decreased from 7 to 5 m^2/g and the pore average diameter increased from 145 to 169 Å (see Tables 1 and 2).

According to SEM–EDX results, V/Ti catalysts prepared by TS (V*x*/Ti TS) and by IWI method (V*x*/Ti IWI) show both a good dispersion of V on titania. Fig. 3 shows elemental analysis map of V and Ti and similar elemental distribution was observed for all other catalysts.

XRD patterns of the catalysts (not shown), clearly present the main reflections attributable to crystalline V_2O_5, in $2\theta = 15^\circ$ (33), 20° (100), 26° (75), 31° (52) and 32° (25), and the supports: ceria (cerianita), niobia, titania (anatase) and alumina (gamma) phases. For the catalysts with low V loading; V2/Nb, V4/Nb, V/Ce and V7/Al–Ti, V_2O_5 reflections were not observed, which can be attributed to small crystallites well dispersed. Additionally, to analyze surface V species on the catalysts, FT-Raman characterization was performed. The spectra of the catalysts and bulk V_2O_5 (not shown) exhibit similar well-defined bands localized at 993, 699, 515, 477, 404, 303, 283, 195 and 143 cm^{-1}. The peak at 993 cm^{-1} is assigned to the terminal V=O vibration of characteristic crystalline V_2O_5. In view of the fact that Raman signal for crystalline V_2O_5 is more intense than that of surface vanadium oxide species, results difficult to assess the presence of surface vanadium oxide species on the catalysts. According to literature reports, the band at 980–1030 cm^{-1} is also assigned to the terminal V=O vibration of the surface metal oxide species [28], corresponding to the presence of metal oxide microcrystals in polymeric species [25]. Then, according to the XRD results we can identify crystalline V_2O_5 and polymeric species, which are well dispersed on supports.

As already mentioned above and according to [24,28,31], the supported vanadium oxide species formed on various supports all essentially possess the same molecular structures. At low surface vanadium oxide loading the supported vanadium oxides are isolated VO_4 units, containing one terminal mono-

Table 3
Textural properties of V_2O_5/TiO_2 catalysts

Catalyst	V_2O_5 (wt.%)	Preparation method	Surface area (m^2/g)	Pore volume (cm^3/g)	Average pore diameter (Å)
V15/Ti TS	15	Thermal spreading	22	0.097	274
V12/Ti TS	12	Thermal spreading	29	0.210	343
V10/Ti TS	10	Thermal spreading	25	0.139	379
V5/Ti TS	5	Thermal spreading	43	0.208	279
V15/Ti IWI	15	Impregnation	18	0.095	353
V10/Ti IWI	10	Impregnation	24	0.163	326

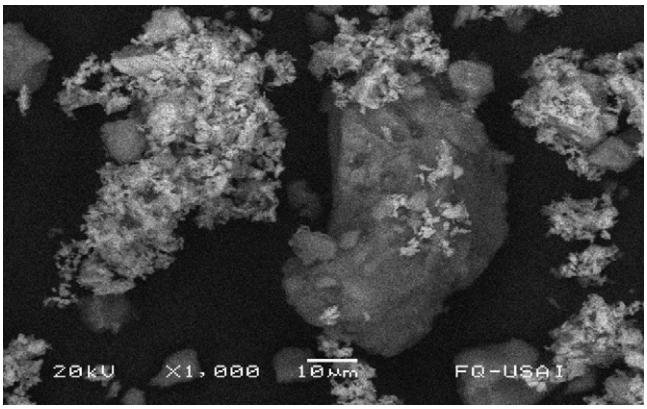

Fig. 1. SEM–EDX micrograph of V/Si–Al.

oxo V=O bond and three bridging vanadium–oxygen–support bond with symmetry C_{3v}. With increasing surface vanadium oxide loading, the amount of dimeric and polymeric chains of VO_4 units will gradually increase. The polymeric vanadium oxide species consist of a terminal V=O bond with one V–O–support and two bridging V–O–V bonds [24]. Similar results have been observed for supported vanadia catalysts [31], which contain the same surface vanadia species independent of the synthesis method after prolonged calcination. The absence of a ''preparation memory effect'' is due to the high mobility of V_2O_5 (Tamman temperature of 370 °C) and the strong driving force of the mixed oxide system to lower its surface free energy by forming a monolayer of surface vanadia species, which possesses a low surface free energy, on the high surface free energy oxide support. In the case of silica, the surface vanadia species can be segregated, due to repulsion between silica and vanadia [31].

Temperature-programmed reduction (TPR) has provided very useful information on the nature and the strength of the interaction between supported species and support, and it has been shown to be a sensitive technique for studying reducibility of V species [32]. Fig. 4 shows the TPR profiles of some catalysts. Thermal conductivity detector (TCD) signal of TPR experiments is calibrated by reduction of a high purity V_2O_5 sample, which is precisely the active phase of these catalysts and it was taken as reference. Bulk V_2O_5 exhibits a well-defined reduction peak from 450 to 850 °C, with temperature of reduction rate maximum (T_{max}) at 645 °C [18]. This peak is associated to the reduction of V(+5) to V(+3) species [32]. The catalysts exhibit a similar reduction peak, but at lower temperatures (T_{max} are presented in Table 4) and the reduction starts, depending on the catalysts, between 300 and 400 °C. These temperature shifts can be attributed to presence of more easily reducible highly dispersed V species on surface, and the V species–support interaction. TPR quantitative results in Table 4 show that the reduction degree is very high in these catalysts (more than 89%) and, it depends on the support and V loading. For V*x*/Al–Ti, if V loading increases: the reduction degree decreases and T_{max} remains practically constant. While

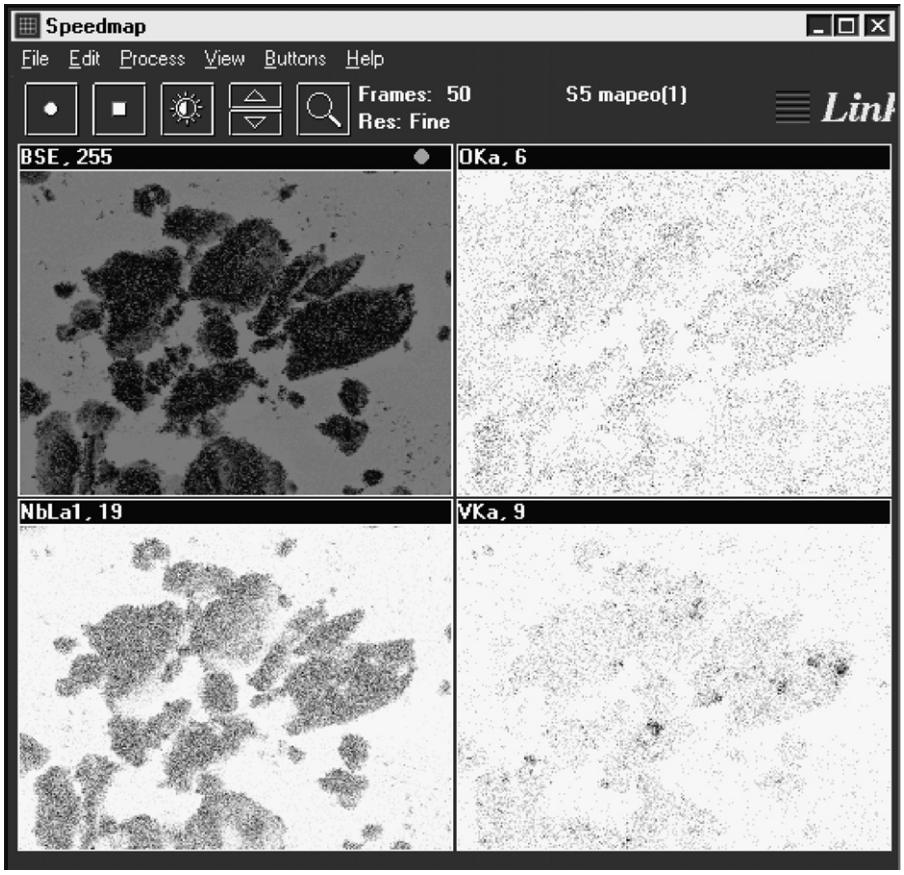

Fig. 2. SEM–EDX micrograph of V6/Nb, with elemental analysis map of V, O and Nb.

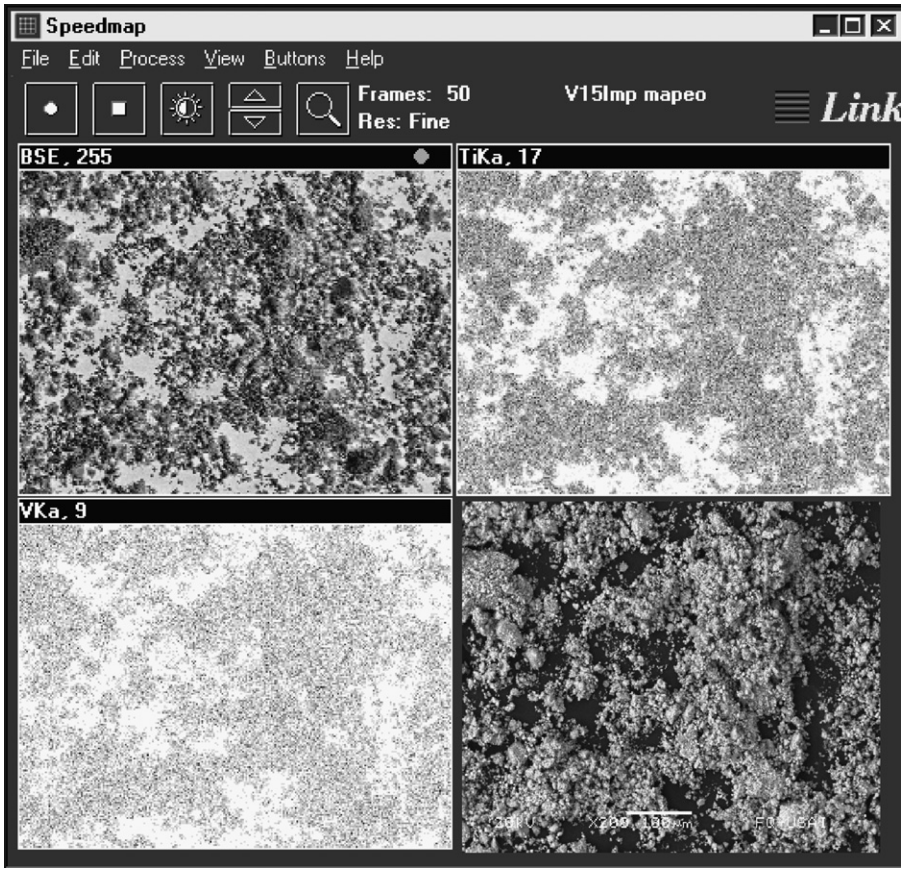

Fig. 3. SEM–EDX micrographs of V15/Ti IWI, with elemental analysis map of V and Ti.

for V*x*/Nb, the reduction degree is higher for V6/Nb and T_{max} is the lowest for this catalyst. Then V species dispersion and the interaction of V species–support delineate the V reduction. The TPR profiles of catalysts with the same V loading, prepared by TS or IWI method, were similar at the same T_{max} (not shown), and only a slight difference in the reduction degree was obtained (see V15/Ti in Table 4). This is attributed to calcination treatment of supported vanadium oxide catalysts, which produces essentially the same vanadium oxide species [26]. Reducibility trend obtained for the catalysts with similar surface coverage of V was: V19/Al (98.6) > V15/Al–Ti (96.9) > V6/Nb (96.2) > V12/Ti (91.8) ∼ V6/Ce (91.6). These results suggest that the reduction of the surface vanadia species is influenced by the specific oxide support taking into account a similar superficial vanadium loading.

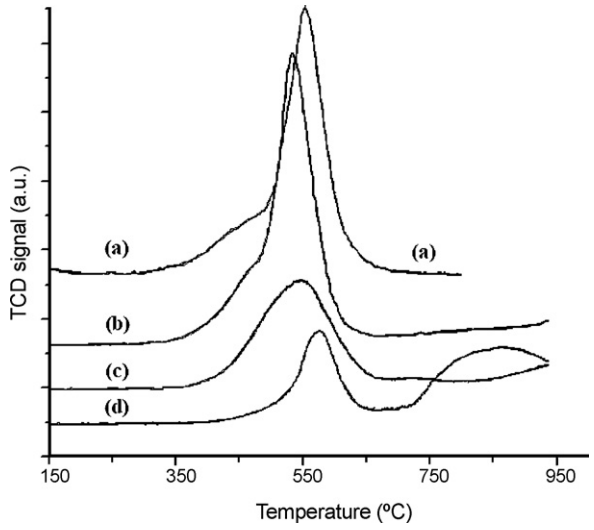

Fig. 4. TPR patterns of: (a) V19/Al, (b) V15/Al–Ti, (c) V12/Ti and (d) V6/Ce.

3.2. Oxidesulfurization of DBTs in presence of V-based catalysts

The reactive system consists of two liquid phases, diesel and extraction solvent, and a solid catalyst. Hence, we will present the results obtained from the GC-analysis of the diesel phase, to evaluate the total removal of DBTs. The solvent phase will be analyzed in order to evaluate the fraction extracted and sulfone yields of DBTs. Fig. 5 shows the total sulfur removal, extraction and yield to DBT sulfone, obtained at 60 °C with H_2O_2 and V19/Al, as catalyst. Total sulfur removal is the fraction of DBTs eliminated from the diesel phase respect to initial concentration in the feedstock. This result shows that it is possible to remove very high percentages of DBTs in a few minutes and mild conditions. DBT-compounds, which contribute mainly to the sulfur compounds in diesel, are removed in about 30 min. Extraction was defined as the fraction of DBTs detected in the solvent phase respect to the initial concentration in the feedstock. With all catalysts, the DBTs extracted reach a

Table 4
Quantitative results of TPR

Catalyst	V_2O_5 loading (μmol)	H_2 consumption (μmol)	Reduction degree (%)	T_{max} (°C)
V19/Al	240.6	474.2	98.6	550
V6/Ce	82.5	151.0	91.6	570
V15/Ti IWI	206.3	381.6	92.5	540
V15/Ti TS	206.3	387.0	93.8	540
V12/Ti TS	164.9	302.9	91.8	545
V7/Al–Ti	103.0	202.8	98.4	530
V15/Al–Ti	206.2	399.5	96.9	530
V22/Al–Ti	309.3	583.9	94.4	535
V2/Nb	27.5	50.0	89.1	590
V4/Nb	54.9	105.9	94.4	600
V6/Nb	82.5	159.7	96.2	570
V10/Nb	137.5	201.5	95.8	610
V20/Nb	274.9	251.7	89.2	635

maximum within the first minutes and subsequently decrease as reaction time continues. As sulfones were obtained only in solvent phase, these profiles describe a consecutive process scheme [17], being the extracted DBTs the intermediate ''product'':

$$DBTs_{(diesel)} \rightarrow DBTs_{(solvent)} \rightarrow sulfone_{(solvent)}.$$

The oxidation of sulfur compounds with *t*-butyl hydroperoxide (TBHP) and H_2O_2 was carried out at 60 °C, using the support as catalyst. With some of the supports used, the corresponding sulfone yields are shown in Table 5. These supports present low ODS activity and their activity differences cannot be correlated to surface area (see Table 1). Otsuki et al. [20] evaluated similar materials as catalysts, for ODS of middle distillate using *t*-butyl hypochlorite as oxidant, and they obtained relatively high activities (50–94%) which correspond to the order of acidity of these oxides: alumina > titania ∼ silica. Wachs et al. [31] reported that the Lewis acidity of these oxides is alumina > niobia > titania, then in our study the ODS activity does not correspond to these acidity trends using neither H_2O_2 nor TBHP.

Tables 6 and 7 show the ODS results obtained in 30 min with all V-based catalysts at 60 °C in presence of H_2O_2 as oxidant.

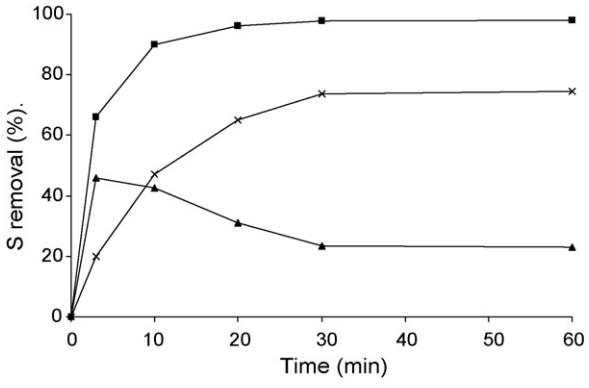

Fig. 5. DBT removal (■), extraction (▲) and sulfone yield (×) profiles in function of reaction time, at 60 °C in presence of V19/Al and H_2O_2 as oxidant.

With these catalysts three issues were evaluated: preparation method, V loading and support effect. To compare the preparation method, V*x*/Ti (*x* = 10 and 15 wt.%) were prepared by thermal spreading (TS) and incipient wetness impregnation (IWI). The total S-removal obtained (Table 6) is similar with both methods, but the sulfone yield with V10/Ti TS is clearly higher than that obtained with V10/Ti IWI. Then, TS method presents slight advantages over IWI method, because it is very simple to achieve and can increase ODS activities. Since the calcination time during catalyst preparation was the same for both methods, it could have not been enough to achieve the same distribution of vanadium species, given that vanadium precursor used in IWI method was reduced upon dissolution in oxalic acid and subsequently reoxidized to V_2O_5 during calcination.

As it was stated above, catalytic supports show very low activity (Table 5), but when vanadia was dispersed on it, an important increase in ODS activity was observed. These results revealed that V species act as active phase in the oxidation of DBTs to DBTs sulfones. For every catalyst, the oxidation activities increased with increasing V loading up to an equivalent V monolayer: V12/Ti, V15/Al–Ti and V6/Nb (Table 6). Above this content the oxidation activities slightly decreased; this may be attributed to the amount of dimeric and polymeric chains of VO_4 units, which gradually increase and form polymeric vanadium oxide species. For V*x*/Nb catalysts, although the highest total S-removal is obtained with V20/Nb, the sulfone yield of DBTs increased with V content up to 6 wt.% and decreased when V content was beyond this value.

Table 5
Sulfone yields (%) obtained at 60 °C and 30 min, using a catalytic support as catalyst, in presence of H_2O_2 or TBHP as oxidant

	H_2O_2			TBHP		
	Alumina	Titania	SBA-15	Alumina	Titania	Niobia
BTO_2	8.1	8.8	0.0	9.3	4.6	4.3
$DBTO_2$	9.4	17.2	3.8	14.8	14.4	5.6
4-$MDBTO_2$	4.9	5.4	1.3	12.8	12.3	5.1
4,6-$DMDBTO_2$	2.5	2.4	0.6	10.2	9.7	4.8

Table 6
Total removal and sulfone yield of DBTs in 30 min with several catalysts at 60 °C in presence of H_2O_2 as oxidant

Catalyst	ODS (%)	BT	DBT	4-MDBT	4,6-DMDBT
V5/Ti TS	Total removal	83.5	94.5	84.5	68.3
	Sulfone yield	15.6	53.5	36.9	24.2
V10/Ti TS	Total removal	85.8	95.9	91.4	75.8
	Sulfone yield	6.5	56.1	39.5	25.4
V12/Ti TS	Total removal	87.4	99.5	99.0	95.0
	Sulfone yield	29.4	61.1	53.3	40.3
V15/Ti TS	Total removal	86.7	97.1	96.9	87.6
	Sulfone yield	15.7	56.4	46.4	30.6
V10/Ti IWI	Total removal	82.9	96.1	90.3	74.3
	Sulfone yield	8.8	38.9	28.8	19.2
V15/Ti IWI	Total removal	86.1	98.2	97.1	88.1
	Sulfone yield	20.1	53.8	46.9	33.6
V7/Al–Ti	Total removal	87.6	91.9	94.9	84.9
	Sulfone yield	15.9	49.0	36.8	22.0
V15/Al–Ti	Total removal	87.7	97.9	98.1	91.5
	Sulfone yield	15.4	28.4	25.4	18.5
V22/Al–Ti	Total removal	83.9	94.0	94.3	81.1
	Sulfone yield	11.5	37.1	28.0	10.7
V5/Si	Total removal	53.2	92.2	99.2	58.4
	Sulfone yield	12.8	31.1	24.8	16.5
V10/Si	Total removal	59.8	92.7	98.3	65.1
	Sulfone yield	35.3	70.6	56.9	40.3
V2/Nb	Total removal	89.3	88.2	91.4	81.6
	Sulfone yield	12.0	56.3	38.3	24.7
V4/Nb	Total removal	88.9	84.7	96.2	89.6
	Sulfone yield	32.1	69.8	60.3	45.8
V6/Nb	Total removal	84.6	88.2	96.4	87.7
	Sulfone yield	31.5	78.7	66.2	48.9
V10/Nb	Total removal	88.6	90.6	98.4	92.6
	Sulfone yield	30.9	60.7	55.0	43.0
V20/Nb	Total removal	94.5	97.7	98.5	94.8
	Sulfone yield	24.7	57.3	45.9	30.4

Respect to support effect, sulfone yields of the catalysts with similar vanadia-superficial content are shown in Table 7. These results show that V catalysts supported on alumina (V/Al) and niobia (V/Nb) present higher catalytic activity. All supports used have different physicochemical properties, such as; acidity, isoelectric point (or point of zero charge), reducibility, surface area and pore volume. Even for Al–Ti mixed oxide, which is substantially different from the pure titania and alumina [29], since it has high Ti loading (95%), with Ti into the alumina matrix and a higher proportion of linkages Ti–O–Ti, also with some titania–anatase crystallites on surface. However, ODS activity of vanadia supported catalysts does not show any correlation with these properties, except with V_2O_5 reducibility. This tendency is more evident with V*x*/Nb series, where the activity (sulfone yield) and reducibility are the highest for V6/Nb (see Tables 4 and 7). In an attempt to explain these results, the probable reaction mechanisms must be addressed. According to Sheldon and coworkers [33–36], there are three possible mechanisms for liquid phase oxidations with transition metals, one of them involving an homolytic pathway and the others involving heterolytic routes. The homolytic pathway proceeds via free radical mechanism where in the first step metal active species participates in homolytic cleavage of O–O bond in hydrogen peroxide forming $^{\bullet}OH$ radicals, which are intermediates in homo or heterolytic oxygen transfer processes. Heterolytic routes proceed via oxometal or peroxometal species as active oxidant. Only the latter does not involve a change in the oxidation state of the metal species. Overberger and Cummins [37], and Bateman and Hargrave [38] postulated that the sulfur is oxidized by a nucleophilic attack on a peroxidic complex. Further, Mashio et al. [39] proposed a model presenting the initial stage of the complex formation between the hydroperoxide and catalyst. Discriminating among these three mechanisms depends on the characteristics of the active metal employed. In the case of vanadium (V), all three routes are possible, being the peroxometal pathway the most common in S-compounds oxidation [34]. Regarding our TPR results, Ziolek [40] states that reducibility is a significant parameter in the oxometal pathway and in the radical mechanism, yet it is not possible to assume that the peroxometal pathway is not involved in our ODS system. In summary, the catalyst promotes the creation of oxidant reactive species, which react with DBTs to produce DBTs sulfoxide, and further oxidation produces the corresponding sulfone. For this reason, ODS activity depends on the oxidant decomposition capacity of the catalysts, which is not function of the textural properties.

On the other hand, it has been reported that Mo catalysts supported on SiO_2–Al_2O_3 and TiO_2 show lower oxidation activity compared with that supported on Al_2O_3 [13]. Similarly, our results may be explained by the difference in polarity of the V–O bond on different supports [24,28,31]. Since there are fewer

Table 7
Sulfone yield (%) of benzothiophenic compounds at 60 °C in 30 min

	V19/Al	V12/Ti TS	V6/Ce	V15/Al–Ti	V22/Al–Ti	V6/Nb
ODS in absence of indole						
BTO_2	37.2	29.4	19.2	15.4	11.5	31.5
$DBTO_2$	73.7	61.1	39.5	28.4	37.1	78.7
4-$MDBTO_2$	67.0	53.3	24.8	25.4	28.0	66.2
4,6-$DMDBTO_2$	52.9	40.3	16.0	18.5	10.7	48.9
ODS in presence of indole (200 ppm)						
BTO_2	22.0	25.7	7.7	20.9	24.7	21.1
$DBTO_2$	57.6	61.2	35.5	43.8	52.1	56.2
4-$MDBTO_2$	42.5	50.1	20.9	37.0	44.6	47.4
4,6-$DMDBTO_2$	27.6	35.7	12.7	26.4	20.5	34.9

unsaturated sites on Al_2O_3–TiO_2 and TiO_2 compared with those on Al_2O_3, it can be inferred that a lower polarity of V–O bond was obtained on SiO_2–Al_2O_3, SiO_2, CeO_2 and TiO_2, leading to lower oxidation activity. According to the reducibility differences observed in TPR, where the reduction of the surface vanadia is influenced by the oxide support. Also, the oxidation activity of DBT increased with V content up to monolayer and decreased when V content was beyond this value, indicating that V dispersion on niobia or Al–Ti was maintained up to this value and the monolayer dispersion is no longer maintained above this value. Therefore, the decrease in the activity for the catalyst with higher V content can be attributed to differences in dispersion of V on these supports, inhibiting the coordination of V–O bond and leading to lower polarity of V–O bond.

Alternatively, in order to evaluate the ODS activity in presence of N-compounds we choose indole as probe molecule because it inhibits the ODS activity of DBTs and can be oxidized in presence of V_2O_5/Al_2O_3 [18]. The results obtained with some V-based catalysts are presented in Table 7, which shows that ODS activity is diminished appreciably with V/Al and V/Nb, and slightly with V/Ti and V/Ce. For example, DBT sulfone yield decreases in 28% (from 73.7 up to 57.6%) with V/Al, and 40% (from 78.7 to 56.2%) with V/Nb, while with V/Ti it is practically constant (61.1%) and with V/Ce is 11% (39.5–35.5%). On the contrary, with V15/Al–Ti, the ODS activity is considerably increased from 28.4 up to 43.8% of DBT sulfone yield (54%). Although V*x*/Al–Ti showed good performance, its ODS activity is lower than V/Ti, V/Al and V/Nb, in decreasing order. Then, with V_2O_5/TiO_2 catalyst the performance is the highest in presence of indole, in spite of its activity in absence of indole is not the highest.

3.3. Reactivities of model sulfur compounds

It has been reported that methyl substitution at 4- and 6-position of DBT remarkably retards the rate of HDS and thus, that 4-MDBT and 4,6-DMDBT are very difficult to convert due to steric-hindrance [1,2]. Namely, the HDS reactivities of DBTs decrease in the order of BT > DBT > 4-MDBT > 4,6-DMDBT. In contrast, ODS reactivity of the sulfur compounds decreases in the order of DBT > 4-MDBT > 4,6-DMDBT > BT (Tables 6 and 7), which is very different from the result commonly obtained with homogeneous catalysts [3,5,7,10], but in accordance to ODS with solid catalysts [13,21]. The fact that BT remained the most difficult to be oxidized can be explained by the much lower electron density of sulfur atom in BT compared with those in DBTs [10]. Oxidation reactivity differences, regarding DBT and alkyl-DBT, using liquid and solid catalysts are ascribed to steric hindrance [13]. This ODS reactivity trend has also been observed in some other liquid catalyzed systems, where the oxidant species formed have large molecular size, as stated by Te et al. [12] and Murata et al. [9].

3.4. Oxidesulfurization of Mexican diesel fuel

Since V/Al, V/Ti and V/Al–Ti catalysts present high performance (Table 7), ODS of actual diesel was carried out on these catalysts to study the oxidation reactivity of DBTs compounds prevailing in hydrotreated diesel. ODS process was applied to the Mexican diesel fuel, and Figs. 6–10 show the GC–FID and sulfur-specific GC–PFPD analyses. FID analyses of the original diesel before and after the catalytic oxidation show that the chromatogram traces were almost the same as those of the original diesel (Fig. 6), and there are no significant changes in either distribution or intensity of these peaks. Diesel consisted basically of paraffinic hydrocarbons (C9–C25) as shown by a series of spike peaks. In minor proportion aromatic compounds were found, such as alkyl-substituted naphtalenes, bipheniles, benzenes, fluorene, anthracene, phenanthrene and xylenes.

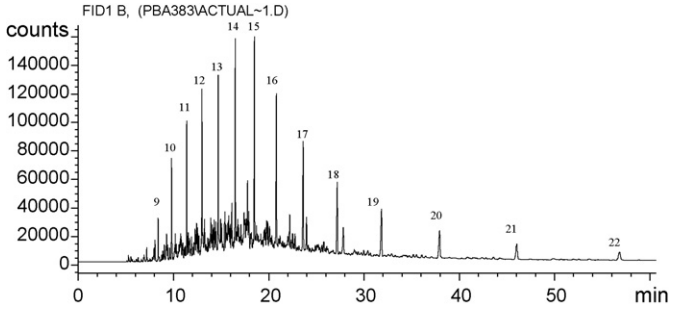

Fig. 6. GC–FID chromatogram of the original or oxidesulfurized diesel.

During ODS process, GC-peaks of DBTs almost disappeared (diesel phase) and the peaks of DBT sulfones appeared after oxidation in solvent phase, indicating that the oxidation of DBTs was leading to the formation of DBT sulfones. These results show that all sulfur-containing compounds can be significantly oxidized to sulfones at 60 °C in 30 min and the

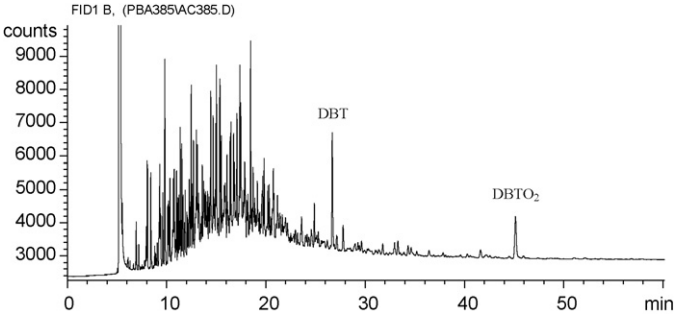

Fig. 7. GC–FID chromatogram of solvent phase after ODS of the diesel, with additional DBT (450 ppm of S).

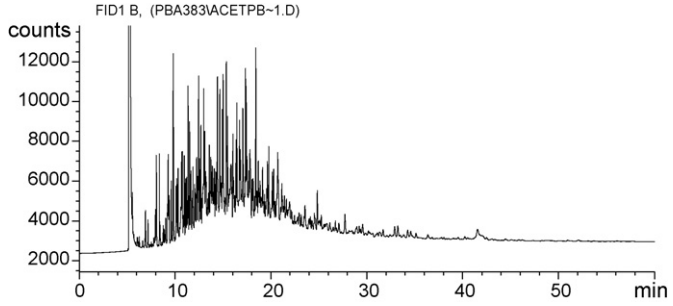

Fig. 8. Solvent-phase chromatogram (FID) after physical extraction. Using actual diesel with total sulfur content of 350 ppm.

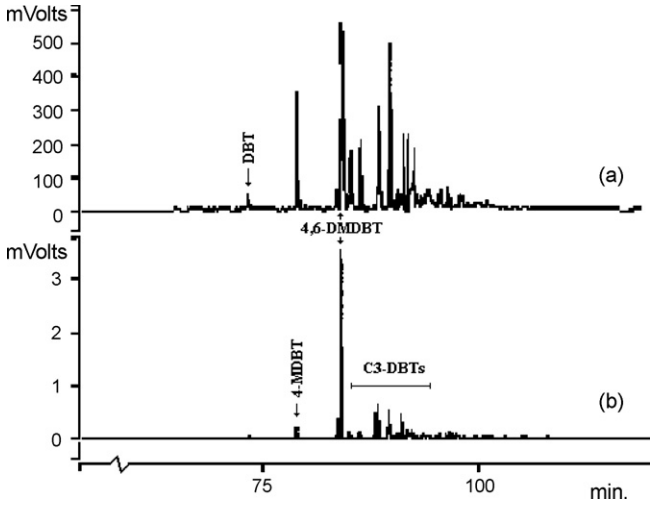

Fig. 9. Sulfur-specific chromatograms (PFPD) of (a) original and (b) oxidesulfurized diesel. Notice the scales are different.

main sulfur compound remaining in diesel was 4,6-DMDBT, which is very difficult to be desulfurized. Fig. 7 shows a chromatogram of extraction-solvent phase after ODS, there we can observe the extraction of both aromatic compounds and DBTs, and well-defined peaks of DBT sulfone. In this test, we added DBT (450 ppm S) into diesel in order to obtain more evident results.

Without catalyst, no oxidation of DBTs was observed indicating that the catalyst was necessary for oxidation of DBTs to DBT sulfones with H_2O_2 at these conditions. However, physical extraction of DBTs and aromatics was observed. Fig. 8 shows the chromatogram of the solvent phase after extraction process without catalysts and H_2O_2, which is similar to Fig. 7, except for the peaks of DBT and DBT sulfone.

PFPD is a specific detector for S-compounds, with this detector species found in fuel were DBT and alkyl-substituted dibenzothiophenes. These refractory species have been reported to make deep desulfurization of fuels difficult to meet the more stringent regulation [1,2]. In Fig. 9, GC–PFPD chromatograms showed the distribution of DBTs before and after ODS reaction. It is seen that a cluster of peaks exists in the original diesel between 85 and 95 min, which correspond to alkyl-substituted DBT (C3-DBTs). After oxidation, the whole group of peaks disappeared (notice the scales are different), mainly prevailing small amounts of 4,6-DMDBT. There are two mayor S-compounds left in the desulfurized diesel, 4-MDBT and 4,6-DMDBT, and in minor proportion C3-DBTs, which are the most refractory compounds under ODS conditions. But it is evident after ODS reaction that there was a noticeable decrease in the amounts of these S-compounds, including 4-MDBT and 4,6-DMDBT.

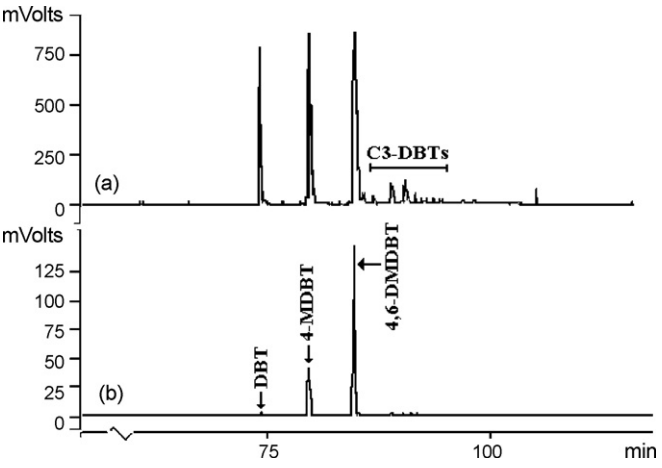

Fig. 10. Sulfur-specific chromatograms (PFPD) of (a) original with additional DBTs (655 ppm) and (b) oxidesulfurized diesel. Notice the scales are different.

Original diesel has 350 S-ppm, but in order to evaluate more precisely the ODS reactivity of DBTs in these conditions, 656 S-ppm of DBT (279), 4-MDBT (195) and 4,6-DMDBT (182) were added into diesel and ODS reaction was carried out with V22/Al–Ti at 60 °C. Fig. 10 shows S-specific chromatograms of diesel before and after 30 min reaction, where we can observe the peak evolution of DBTs, prevailing small amount of 4-MDBT and 4,6-DMDBT, in contrast DBT practically disappeared. These findings are also consistent with the order of oxidation reactivity of the model sulfur-containing compounds in hexadecane, the oxidation reactivities decreased as follows: DBT > 4-MDBT > 4,6-DMDBT > BT. The results of the best run indicated that ODS produced desulfurized diesel with S-content as low as 10 ppm, which corresponds to overall S-removal of 99% after 30 min reaction at 60 °C. Then V-based catalysts have high catalytic activity for all kinds of sulfur-containing compounds present in actual diesel, and DBTs compounds prevailing in diesel can be removed efficiently by oxidation and extraction with a polar aprotic solvent, such as acetonitrile.

During ODS process there are no significant changes in either distribution or intensity of paraffinic hydrocarbon (C9–C25) peaks in the original and desulfurized diesel (Fig. 6). It indicates that these compounds were not subject to any negative effects. However, the intensity of aromatic compounds decreased slightly due to extraction (Figs. 7 and 8). It reveals that aromatic compounds have relatively higher polarity than saturated hydrocarbons and intend to partition into extraction solvent. But nonetheless this portion of aromatics can be easily recovered by distillation of solvent [41].

The efficiencies of oxidative desulfurization of diesel were up to 99% and the sulfur concentration of diesel after desulfurization can drop to 10 ppm. These results suggest that ultra-deep desulfurization of diesel can be achieved by ODS process in presence of vanadia-based catalysts. Using this process as a second stage after existing HDS unit, taking a low sulfur diesel (∼500 ppm) down to ultra low-sulfur diesel levels.

4. Conclusions

Vanadia on titania catalysts were prepared by thermal spreading (TS) and incipient wetness impregnation (IWI) method, and according to SEM–EDX, XRD and Raman FT-IR a good V dispersion was obtained for all catalysts, while the ODS activity was slightly increased with TS method. Vanadia on ceria, alumina or alumina–titania mixed oxides were

prepared by TS method. However for silica-based supports (silica–alumina and SBA-15), the catalysts present V_2O_5 segregation and TS method is not useful for these supports.

ODS of DBTs was conducted in presence of V_2O_5 on several supports. Results showed that total S-removal is close to 99% using vanadia on titania as catalyst and this decreased according to the support used in the next order: alumina > titania > niobia > Al–Ti mixed oxide > SBA-15. While the oxidation activity of DBTs for V catalyst supported on niobia or alumina presented higher catalytic activity than all the other catalysts (niobia > alumina > SBA-15 > titania > ceria > Al–Ti mixed oxide), in presence of a N-compound as indole the best catalytic performance is obtained with titania-supported catalysts.

For all catalysts and fuels used, the results indicated that the oxidation reactivity of sulfur compounds prevailing in diesel decreased in the order of DBT > 4-MDBT > 4,6-DMDBT > BT, which indicates that steric hindrance of alkyl groups substituted in 4- and 6-position of DBT is taking place.

ODS of actual Mexican diesel fuel (with 350, 800 and 1005 ppm of total S) were up to 99% and the sulfur level diminishes less to 10 ppm. Consequently, ultra-deep desulfurization of diesel can be achieved by ODS process in presence of vanadia-based catalysts.

Acknowledgements

The authors thank DGAPA-UNAM (IN-100406) for financial support. H. Gomez wishes to acknowledge CONACYT for her scholarship. Technical assistance of I. Puente (SEM–EDX) and A. Gutierrez (FT-IR Raman) is gratefully acknowledged.

References

[1] I.V. Babich, J.A. Moulijn, Fuel 82 (2003) 607.
[2] C. Song, Catal. Today 86 (2003) 211.
[3] T. Aida, D. Yamamoto, M. Iwata, K. Sakata, Rev. Heteroatom Chem. 22 (2000) 241.
[4] S.E. Bonde, W. Gore, G.E. Dolbear, Am. Chem. Soc., Div. Pet. Chem. 44 (1998) 199.
[5] F.M. Collins, A.R. Lucy, C. Sharp, J. Mol. Catal. A: Chem. 117 (1997) 397.
[6] D. Chapados, W.L. Gore, S.E. Bonde, G. Dolbear, E. Skov, Annual Meeting NPRA Paper No. AM-00-25 (2000).
[7] I. Funakoshi, T. Aida, European Patent 0565324A1 (1993).; US Patent 5,753,102 (1998).
[8] V. Hulea, F. Fajula, J. Bousquet, J. Catal. 198 (2001) 179.
[9] S. Murata, K. Murata, K. Kidena, M. Nomura, Energy Fuels 18 (2004) 116.
[10] S. Otsuki, T. Nonaka, N. Takashima, W. Qian, A. Ishihara, T. Imai, T. Kabe, Energy Fuels 14 (2000) 1232.
[11] Y. Shiraishi, T. Hirai, Energy Fuels 18 (2004) 37.
[12] M. Te, C. Fairbridge, Z. Ring, Appl. Catal. A: Gen. 219 (2001) 267.
[13] D. Wang, E.W. Qian, H. Amano, K. Okata, A. Ishihara, T. Kabe, Appl. Catal. A: Gen. 253 (2003) 91.
[14] F. Zannikos, E. Lois, S. Stournas, Fuel Process. Technol. 42 (1995) 35.
[15] T. Aida, D. Yamoto, Am. Chem. Soc. Div. Fuel Chem. 39 (1994) 663.
[16] L. Cedeño, E. Hernandez, F. Pedraza, F. Murrieta, Catal. Today 107 (2005) 564.
[17] H. Gomez, L. Cedeño, Int. J. Chem. Reactor Eng. 3 (2005) A28 http://www.bepress.com/ijcre/vol3/A28.
[18] L. Cedeño Caero, J.F. A. Navarro, A. Gutierrez-Alejandre, Catal. Today 116 (2006) 562.
[19] E. Ito, J.A. Rob van Veen, Catal. Today 116 (2006) 446.
[20] S. Otsuki, T. Nonaka, W. Qian, A. Ishihara, T. Kabe, Sekiyu Gakkaishi 44 (2001) 18.
[21] A. Ishihara, D. Wang, F. Dumeignil, H. Amano, E.W. Qian, T. Kabe, Appl. Catal. 279 (2005) 279.
[22] D. Zhao, Q. Huo, J. Feng, B.F. Chmelka, G.D. Stucky, J. Am. Chem. Soc. 120 (1998) 6024–6036.
[23] R. Gomez, J. Ramirez, R. Nares, R. Luna, F. Murrieta, Catal. Today 107 (2005) 926.
[24] B.M. Weckhuysen, D.E. Keller, Catal. Today 78 (2003) 25.
[25] D.A. Bulushev, L. Kiwi-Minsker, A. Renken, Catal. Today 57 (2000) 231.
[26] T. Machej, J. Haber, A.M. Turek, I.E. Wachs, Appl. Catal. 70 (1991) 115.
[27] E.P. Reddy, R.S. Varma, J. Catal. 221 (2004) 93.
[28] J.P. Dunn, H.G. Stenger, I.E. Wachs, Catal. Today 51 (1999) 301.
[29] J. Ramirez, L. Ruiz, L. Cedeño, V. Harle, M. Vrinat, M. Breysse, Appl. Catal. 93 (1993) 163.
[30] M. Ziolek, Catal. Today 78 (2003) 47.
[31] I.E. Wachs, B.M. Weckhuysen, Appl. Catal. A: Gen. 157 (1997) 67.
[32] I.E. Wachs, Y. Chen, J. Jehng, L.E. Briand, T. Tanaka, Catal. Today 78 (2003) 13.
[33] R.A. Sheldon, J. Mol. Catal. 7 (1980) 107.
[34] I.W.C.E. Arends, R.A. Sheldon, Appl. Catal. A: Gen. 212 (2001) 175.
[35] I.W.C.E. Arends, R.A. Sheldon, H.E.B. Lempers, Catal. Today 41 (1998) 387.
[36] I.W.C.E. Arends, R.A. Sheldon, M. Wallau, U. Schuchardt, Angew. Chem. Int. Ed. Engl. 36 (1997) 1144.
[37] C.G. Overberger, R.W. Cummins, J. Am. Chem. Soc. 75 (1953) 4250.
[38] L. Bateman, K.R. Hargrave, Proc. Roy. Soc. A 224 (1954) 389.
[39] F. Mashio, S. Kato, Yuki Gousei Kagaku 26 (1968) 367.
[40] M. Ziolek, Catal. Today 90 (2004) 145.
[41] H. Mei, B.W. Mei, T.F. Yen, Fuel 82 (2003) 405.